Environmental Science & Technology

Article

pubs.acs.org/est

Comparing Natural Gas Leakage Detection Technologies Using an Open-Source "Virtual Gas Field" Simulator

Chandler E. Kemp, Arvind P. Ravikumar, and Adam R. Brandt*

Department of Energy Resources Engineering, Stanford University, 367 Panama Street, Stanford, California 94305, United States

Supporting Information

ABSTRACT: We present a tool for modeling the performance of methane leak detection and repair programs that can be used to evaluate the effectiveness of detection technologies and proposed mitigation policies. The tool uses a two-state Markov model to simulate the evolution of methane leakage from an artificial natural gas field. Leaks are created stochastically, drawing from the current understanding of the frequency and size distributions at production facilities. Various leak detection and repair programs can be simulated to determine the rate at which each would identify and repair leaks. Integrating the methane leakage over time enables a meaningful comparison between technologies, using both economic and environmental metrics. We simulate four existing or proposed detection technologies: flame ionization detection, manual infrared camera, automated infrared drone, and distributed detectors. Comparing these four technologies, we found that over 80% of simulated leakage could be mitigated with a positive net present value, although the maximum benefit is realized by selectively targeting larger leaks. Our results show that low-cost leak detection programs can rely on high-cost technology, as long as it is applied in a way that allows for rapid detection of large leaks. Any strategy to reduce leakage should require a careful consideration of the differences between low-cost technologies and low-cost programs.

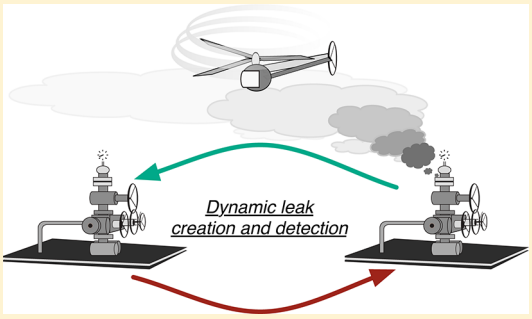

INTRODUCTION

Fugitive methane (CH_4) emissions from the natural gas system are an important source of anthropogenic greenhouse gases (GHGs),[1] representing ≈25% of U.S. CH_4 emissions. In extreme cases, fugitive emissions could offset the climate benefits of switching from other fossil fuels to natural gas.[2,3] Leak detection and repair (LDAR) programs aim to reduce fugitive CH_4 emissions while providing additional revenue to natural gas producers from the sale of recovered gas. LDAR is an area of active research, and many proposed LDAR concepts rely heavily on new technologies, including constant monitoring of gas wells with high-precision methane sensors,[4,5] automated surveys of natural gas fields based on infrared (IR) camera technology,[6] or remote sensing of methane plumes using aircraft or satellites.[7,8]

While many LDAR concepts and technologies have been studied in the literature, less work has been performed to rigorously compare different proposed LDAR programs regarding their effectiveness. For example, which LDAR technology has the most potential to reduce the cost of CH_4 mitigation, or how important is labor minimization in driving cost reductions from a new LDAR concept? Rigorously comparing proposed LDAR programs requires a model of leakage from a gas facility as well as a model of how a LDAR program would detect any given leak. Such a model must be able to accurately simulate the evolution of leakage through time under various proposed and implemented LDAR programs. This model must also include all major costs of LDAR programs, such as labor and technology costs. Because no such model currently exists, we developed the Fugitive Emissions Abatement Simulation Toolkit (FEAST) model to explore the effect of various LDAR programs on long-term leakage rates.

In FEAST, CH_4 leaks in a computer-simulated gas field are generated dynamically as the simulation proceeds. Dependent upon the LDAR program under study, the repair rate is calculated using a physics-based model: the concentration of methane downwind of every leak is simulated using a Gaussian plume model, and the specifications of a particular LDAR program are applied to the simulated plume to determine whether or not it is detected. LDAR programs in FEAST are represented by a combination of technology parameters (e.g., survey sensitivity) and implementation parameters (e.g., survey frequency). Given a LDAR program, FEAST finds and fixes leaks appropriately. Integrating the leakage rate through time yields the total amount of lost gas under a particular LDAR program. From assignment of a value to the lost gas and estimation of the cost of maintaining the LDAR program, FEAST estimates the economic value of the LDAR program in net present value (NPV) terms and LDAR program environmental benefits.

Received: December 11, 2015
Revised: March 23, 2016
Accepted: March 23, 2016

DOI: 10.1021/acs.est.5b06068
Environ. Sci. Technol. XXXX, XXX, XXX−XXX

In this paper, FEAST is applied to four conceptual LDAR programs. We first describe the FEAST methodology and LDAR program representations. We then compare our simplified LDAR programs to illustrate their strengths, weaknesses, potential for improvement, and relative value. We conclude with a description of future directions for research.

METHODOLOGY

FEAST is an open-source model programmed in the MATLAB computing environment.[9] FEAST model code and documentation are made open source as the Supporting Information and, thus, can be downloaded and used as desired by the reader.

Markov Model. FEAST simulates leakage from a natural gas field by modeling every potential leaking component in the field using a two-state Markov process: a component may either be in the "leaking" state or in the "robust" state. The simulation time period is broken into discrete time steps, and every component, whether leaking or not, is given a probability of changing state in a given time step. This probability depends upon the LDAR program being simulated and the behavior of the natural gas infrastructure. Note that Markov processes (by definition) do not depend upon behavior history, while in reality, there is some evidence that the probability of leakage from a component depends upon its type and age.[10−13] This is considered further in the Results and Discussion. With more experimental and statistical data, future versions of FEAST could be implemented using higher order Markov chains.

The FEAST Markov model is implemented in three basic steps: gas field initialization, dynamic simulation, and results storage (see Figure 1).

Gas Field Initialization. The initial condition is defined by the number and size of leaks distributed throughout the natural gas field as well as physical characteristics of the gas field that affect the performance of LDAR programs. Physical characteristics include distance between wells, number of potentially leaking components per well, and area at each wellsite that must be searched for leaks.

Several publicly available data sets exist that characterize the leakage from existing gas fields (Table 1). As shown in Table 1, the Fort Worth air quality study[14] (henceforth FWAQS) offers the largest sample of leaks that is publicly available. We calculate the average number of leaks per well found in the FWAQS (≈6) and apply a truncated normal distribution about this average, approximated to the nearest integer, to initialize leaks in FEAST. FEAST then randomly draws the size of each leak from the leaks found in the FWAQS, which have a heavy-tailed size distribution (i.e., log-normal like; large leaks are proportionally more impactful than would be expected in a simple Gaussian size distribution). The result is a randomly generated set of leaks that is statistically similar to the empirical FWAQS data. FEAST can also use other leak size distributions, provided information from a user. It should be emphasized here that there is growing evidence[15,16] of highly skewed leak size distribution in the natural gas infrastructure. The leak sizes used in this model, derived from the FWAQS, represent one such heavy-tailed distribution.

The distance between wells, number of components per well, and other physical features were chosen to be within the range of values found for U.S. natural gas fields (see Table S3.1 and section S3.2.2 of the Supporting Information).

Atmospheric Conditions. The performance of LDAR programs depends upon the environmental conditions surrounding the gas field, such as the wind speed and atmospheric stability. The wind speed is chosen from an empirical distribution suggested by the Advanced Research Projects Agency-Energy (ARPA-E) in the recent Methane Observation Networks with Innovative Technology to Obtain Reductions (MONITOR) challenge.[4] For each time step, one wind speed is selected from this data set at random. The wind direction is chosen from a second empirical wind data set collected at Fort Worth.[21] Once the wind speed has been selected, the stability class is chosen at random with equal probability from the realistic classes associated with that wind speed.[22] See section S3.3 of the Supporting Information for more details. In the absence of site-specific information, the ARPA-E wind speed distribution can be used as a template wind profile near production facilities. Users of this model can input appropriate data sets specific to the infrastructure being studied. It should be noted that meteorological conditions, such as atmospheric conditions, time of day, etc., can play a significant role in detection capability for different technologies. While these can be included in the technology modeling, the results presented in this paper assume daytime operation for all technologies.

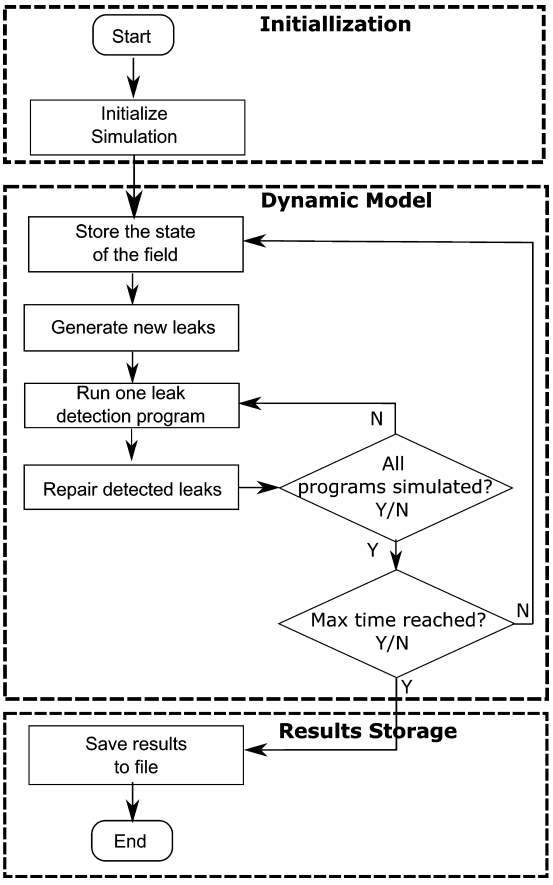

Figure 1. Flowchart of the FEAST model structure.

Dynamic Simulation. At each time step, a small fraction of components in the robust state are changed to the leaking state to emulate a non-zero leak production rate. No published studies were found that directly estimate the leak production rate; however, it is possible to use two existing studies to estimate the rate of leak generation.

First, the Carbon Limits data set[17] (henceforth CL) provides one means for estimating the leak production rate. CL reports data from thousands of wells, suggesting that, within the first

DOI: 10.1021/acs.est.5b06068
Environ. Sci. Technol. XXXX, XXX, XXX−XXX

Table 1. Summary of Results from Leakage Studies of Natural Gas Production Facilities

name	year	detection method	number of wells	number of leaks	leaks per well
Carbon Limits[17] [a]	2014	IR[b] camera	≈5300	NR	NR
Fort Worth[14] [c]	2011	FID[d]/IR camera	1138	2126[e]	≈2
Allen et al.[18]	2013	IR camera	292	769	≈2.6
Kuo[19]	2012	spectroscopy	172	59	≈0.3
API 4589[20]	1993	FID	82	1513	≈18
Fernandez[11]	2006	bubble test	12	132	11

[a]Carbon Limits reported the number of well sites and well batteries surveyed. We estimate the number of wells by assuming an average of three wells per survey in the well sites and well batteries category. There were 39 505 leaks recorded in all facilities. [b]IR = infrared. [c]All components were surveyed with an IR camera. A total of 10% were also surveyed with a FID. [d]FID = flame ionization detector. [e]Data on the number of wells and leaks can be found in the Government of Fort Worth, TX website http://fortworthtexas.gov/gaswells/air-quality-study/final. Site-specific data can be found in Appendix 3-B: Emissions calculations workbook of the Fort Worth, TX Air Quality Study.[14]

year after a leak survey is completed, the average natural gas well battery emits 1.8 tons of volatile organic compounds (tVOC). The associated methane leak creation rate is calculated on the basis of the following four assumptions: (1) Leakage that persists after the LDAR survey is negligible (i.e., leaks that are found in a LDAR survey are fixed). (2) The rate of leakage increases linearly throughout the year. (3) CH_4 and volatile organic compounds (VOCs) mole fractions are consistent with the average values reported by technical documents.[20] (4) The number of leaks repaired between LDAR surveys is negligible.

Using these assumptions, we derive eq 1 for the leak creation rate, where E_{VOC} is the estimated total VOC emissions between surveys, Δt is the length of time between surveys (1 year, in this case), and m_{CH_4}/m_{VOC} is the mass ratio of CH_4 emissions to VOC emissions (see section SA.2 of the Supporting Information for the method used to estimate m_{CH_4}/m_{VOC}). According to eq 1, the CL data suggest a leak creation rate of 3.8×10^{-4} g of CH_4/s per well per day.

$$R_l = \frac{2E_{VOC}}{\Delta t^2}\frac{m_{CH_4}}{m_{VOC}} \quad (1)$$

Alternatively, FWAQS data[14] can be used to estimate the leak production rate. On the basis of the assumption that the rate of leakage increased linearly from zero when the facility was first built, the leak creation rate in the Barnett shale region can be estimated by dividing the total leakage rate in the FWAQS study by the average age of gas wells. This gives a leak production rate of 1.8×10^{-4} g/s per well per day or ≈50% of the CL value. FEAST defaults to the average value of 2.6×10^{-4} g/s per well per day. There are many possible explanations for the discrepancy between the two results reported above, including different types of infrastructure, different facility age, different regulations, or different management practices in the two regions studied. As noted below, more work is needed to generate better estimates of the leak detection rate. To compensate for the lack of reliable data on leak production rates across the U.S. infrastructure, we have used a range from 1.8×10^{-4} to 3.8×10^{-4} g/s per well per day in the sensitivity analysis. Because the model is open-source, these values could be replaced with a more representative generation rate for a particular set of gas wells.

The probability of a component switching from the robust to the leaking state during a time step of duration δt is given by eq 2, where R_l is the leakage creation rate (g/s per well per day), $N_{c/w}$ is the number of components per well, and μ_l is the average leak size (g/s).

$$P_{R,L} = \frac{R_l}{N_{c/w}\mu_l}\delta t \quad (2)$$

At each time step every robust component is given the probability $P_{R,L}$ to begin leaking. Components that begin leaking have leakage rates drawn from FWAQS empirical data, as during initialization.

Choosing a $P_{R,L}$ that is constant through time implies that the quality of gas infrastructure and maintenance does not change during the simulation. It does not imply that the leakage increases linearly through time. On the contrary, the stochastic nature of FEAST allows for a different number of leaks to be introduced at every time step and the size of each created leak is chosen randomly, independent of $P_{R,L}$. Super-emitters are extremely large but rare leaks in the FWAQS, and their frequency in FEAST follows the FWAQS distribution. When FEAST happens to generate a super-emitter, a significant discontinuity occurs in the total field leakage, just as the total leakage from a real gas field suddenly increases if a tank hatch cover is accidentally left open. Over sufficiently long time scales, these discontinuities can be averaged out and the total leakage will increase approximately linearly if $P_{R,L}$ is constant (and repairs are neglected). A small modification to the Markov model can allow for a variable $P_{R,L}$ if a change in the leak production rate is expected. We explore one such scenario in the Results and Discussion.

LDAR Programs. A LDAR program in FEAST includes the combination of an applied LDAR technology and a LDAR implementation. Technology parameters include factors such as detector costs and sensitivities, while implementation parameters include factors such as frequency of surveys or repair practices. The probability that a leaking component switches to the robust state ($P_{L,R}$) in a given time step requires a model of the LDAR program being evaluated. By definition

$$P_{L,R} = P_{L,R}^{null} + P_{L,R}^{LDAR} \quad (3)$$

By default, all LDAR simulations include a "null LDAR program", which contributes $P_{L,R}^{null}$ to the probability of detecting a leak. In the scenarios below, $P_{L,R}^{null}N_L^i = P_{R,L}N_R^i$, where N_L^i and N_R^i are the initial number of leaking and robust components, respectively. That is, the background rate of leak creation multiplied by the number of robust components equals the rate of leak detection multiplied by the number of leaking components without LDAR, and therefore, the number of leaks is in steady state over long-time Markov simulation. Adding a LDAR program on top of the null program increases the value of $P_{L,R}$ by adding additional probability of finding and fixing leaks $P_{L,R}^{LDAR}$, such that a new, lower steady-state leakage

DOI: 10.1021/acs.est.5b06068
Environ. Sci. Technol. XXXX, XXX, XXX−XXX

Table 2. Notable Parameter Settings in the Base Case and Extreme Sensitivity Cases[a]

symbol	name	units	base case	high savings	low savings
		Markov Model			
R_l	leak production rate	g/s per well per day	2.6×10^{-4}	5.2×10^{-4}	1.3×10^{-4}
	leak size data source		FWAQS[14]		Allen[18]
C_g	gas price	$/mcf	5	8	3
R_{RD}	real discount rate	% per year	8	5	10
A	aging factor		1	2	
		FID			
C_{cap}	total capital	$	35000	20000	50000
λ	lifetime	years	10	20	5
R_S	survey speed	components/hour	150	300	75
T_{SI}	survey interval	days	100	200	50
T_{SU}	setup time	hours	0.5		
		DD			
$C_{detector}$	cost per detector	$	500	200	1000
$N_{s/W}$	detectors per well		4	2	8
T_{LI}	repair interval	days	50	25	100
T_{setup}	setup time	hours	0.5		
Φ_{min}	minimum concentration	g/m^3	10^{-2}	10^{-3}	10^{-1}
		MIR			
C_{cap}	capital cost	$	120000	60000	240000
λ	lifetime	years	10	5	20
R_S	survey speed	components/hour	500	1000	250
Γ_{min}	minimum concentration path	m-g/m^3	0.4	0.2	2
$F_{PD,min}$	minimum fraction of pixels above Γ_{min} for detection	%	10	20	5
T_{SI}	survey interval	days	100	200	50
T_{SU}	setup time	hours	0.5		
		AIR			
C_{cap}	total capital cost	$	193000	100000	300000
$F_{PD,min}$	minimum fraction of pixels above Γ_{min} for detection	%	10	5	20
Γ_{min}	minimum concentration path	m-g/m^3	0.4	0.2	2
T_{SI}	survey interval	days	14	7	28
v_S	survey speed	m/s	5	10	2.5
Z_{cam}	camera height	m	20	10	40
λ	lifetime	years	3	6	1.5

[a]See the Supporting Information for a complete list of Markov model and LDAR program specifications.

rate is reached. Changing the settings of the null program allows the user to explore scenarios in which the background prevalence of leaks increases as the facility ages (i.e., $P_{L,R}^{null} N_L^i < P_{R,L} N_R^i$).

Four simplified example LDAR programs are simulated here. These LDAR programs include the following: (1) Flame ionization detector (FID): Manual application of a flame ionization detector technology, after which components with a local CH_4 concentration above a threshold are replaced. The FID technology is the "default" first pass detection technology used in many historical studies. (2) Distributed detector (DD): Methane detectors are placed at intervals along the dominant downwind direction characteristic of the location and alert repair crews when local concentrations at a detector exceed a threshold detection limit. After leaks are detected, repairs are performed at a set repair interval. (3) Manual infrared (MIR): A manual infrared imaging method, wherein an operator uses an IR camera to visualize methane plumes and tags components to be fixed. A manual IR technique is another very commonly applied LDAR method. (4) Automated infrared (AIR): An automated infrared technique where an IR-equipped aircraft flies over natural gas sites and detects leaks from their IR signature. After leaks are detected, images of each leak are sent to repair crews to facilitate repair.

The most important parameters for each LDAR program are given in Table 2. See Tables S3.5–S3.8 of the Supporting Information for full details of LDAR parameters and default settings for each LDAR program.

In the FID survey method, all leaks are found and repaired at each time step when a survey occurs. Therefore, $P_{L,R}^{LDAR} = 0$ at all time steps, except at the time step of a survey when $P_{L,R}^{LDAR} = 1$. Such a detection certainty is justified because the underlying data set used in FEAST was obtained using a FID-based leak detection program.

FEAST uses a Gaussian plume model to compute $P_{L,R}^{LDAR}$ for the DD, MIR, and AIR programs. Such a model accounts for the buoyancy of emitted gas and reflection of the plume off the ground. The effect of an atmospheric inversion is not considered because we are interested in the behavior of plumes within a few tens of meters of the ground. The concentration Φ (g/m^3) downwind of the plume is given by

$$\Phi = \frac{Q}{2\pi u \sigma_y(x)\sigma_z(x)} \exp\left(\frac{(y-y_0)^2}{2\sigma_y^2(x)}\right)\left[\exp\left(\frac{(z-z_M(x))^2}{2\sigma_z^2(x)}\right) + \exp\left(\frac{(z+z_M(x))^2}{2\sigma_z^2(x)}\right)\right] \quad (4)$$

DOI: 10.1021/acs.est.5b06068
Environ. Sci. Technol. XXXX, XXX, XXX−XXX

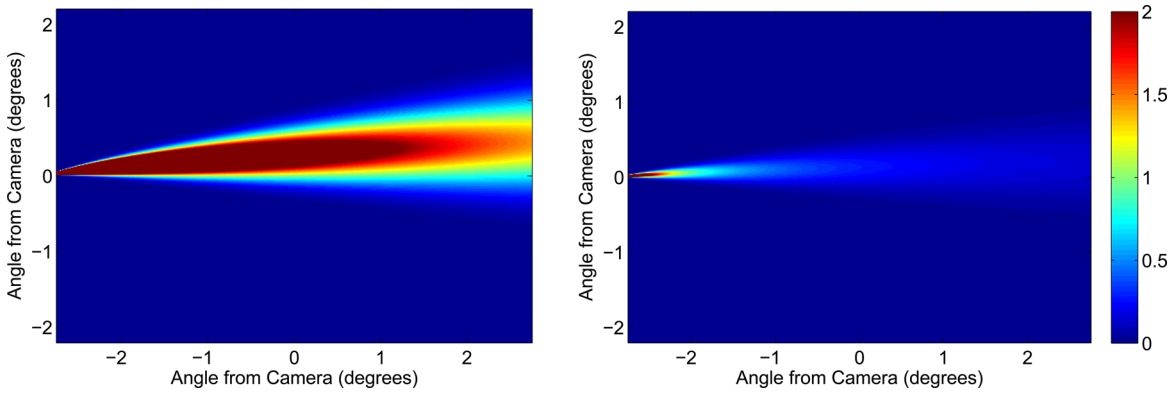

Figure 2. Simulated concentration path length profile of natural gas leaks of (left) 1.5 g/s and (right) 0.15 g/s, at a wind speed of 2 m/s and stability class C. Leaks are imaged by a camera 30 m to the side of the leak source. The color bar indicates the signal-to-noise ratio as imaged by the IR camera.

where x, y, and z are the coordinates at which the concentration is to be calculated (m): x is measured downwind of the leak, z is the vertical displacement from the ground, y_0 is the position of the leak source in the y direction. Q is the leak flux (g/s), and u is the wind speed (m/s). σ_y and σ_z are the standard deviation of the plume concentration (m), extracted using linear interpolation to published curves[22−24] based on the atmospheric stability class. Finally, z_M is the vertical position of the middle of the plume as a function of x. z_M accounts for the plume buoyancy and follows the methodology suggested by Beychok (see section S2.3 of the Supporting Information).[25]

The DD, MIR, and AIR programs use the Gaussian plume model in different ways. For the DD detector, the concentration of methane at the location of the plume is compared to a predefined detection threshold. If the concentration is greater than the threshold, the leak is detected. The probability that the concentration exceeds the detection threshold depends upon the size of the leak, the location of the leak relative to the detector, and atmospheric conditions. The location of the leaks are chosen randomly within a pad area definition. Various placement patterns of DD sensors are explored in prior work.[26]

The detection threshold for the IR camera methods requires that a minimum fraction of the camera pixels be above a minimum concentration path length.[27] The signal in each pixel is estimated by numerically integrating the concentration calculated by the Gaussian plume model along the path imaged by each pixel according to eq 5, where α is an implied constant in the detection criteria and Λ is the path imaged by a pixel.

$$\text{signal} = \alpha \int_{\Lambda} \Phi(x(s), y(s), z(s))\, ds \tag{5}$$

A simulation of this concentration path length, as seen by an IR camera 30 m to the side of the leak source, for two different leak rates, using the Gaussian plume model is shown in Figure 2.

Economic Analysis. The Markov model generates a time series of leakage associated with each simulated LDAR technology. Assigning a value to the gas saved by a LDAR program in comparison to a status quo simulation (in this case, the null LDAR program) enables a NPV analysis of each modeled LDAR program and an estimate of the CH_4 emitted.

We use a standard NPV analysis to compare the economic value of various LDAR programs. The NPV is calculated according to eq 6, where $\mathbb{Z}_t$ is the set of all time steps, $V_L(t_i)$ is the value of the leakage lost during the ith time step, and C is the cost of running the LDAR program in the ith time step. R_{RD} is the real discount rate (8%).

$$\text{NPV} = \sum_{i \in \mathbb{Z}_t} (V_L(t_i) - C(t_i)) \left(\frac{1}{1 + R_{RD}} \right)^{t_i} \tag{6}$$

The price of natural gas for base-case analysis is fixed at $5/mcf over the entire simulation period, while a range from $3 to 8/mcf is used for sensitivity analysis. The cost of fixing leaks is drawn at random from a comprehensive list of over 1600 leaks from a 2006 United States Environmental Protection Agency (U.S. EPA) study,[11] with costs adjusted for inflation. There was no correlation between the measured leak magnitudes in that study and the estimated costs to fix each leak (see Figure S3.14 of the Supporting Information), thereby justifying randomly selecting costs. It should be noted that the NPV analysis performed here is only representative and is best used as a tool to compare various LDAR technologies in terms of its cost-effectiveness instead of absolute dollar terms. Further refinement of this model would need to incorporate enterprise-level information regarding captial structures and specific characteristics of the business model in use.

RESULTS AND DISCUSSION

A FEAST scenario is defined by the user-defined settings, inputs, and underlying data set provided to FEAST. We refer to the results generated by running FEAST once as one realization of a particular scenario. Because FEAST is stochastic, results will change each time FEAST runs a particular scenario. Numerous realizations must be analyzed to understand the implications of a particular scenario.

Figure 3 shows the leakage time series of a single realization of the default scenario in FEAST for different LDAR programs, including the null program and a no-repair program. While the time-series change in total leakage will be different for each realization because of the stochastic nature of the model, the general trends in Figure 3 are characteristic of the LDAR programs. This simulation covers a 10 year time period; therefore, the number of evaluation periods is large, and steady-state behavior is always reached. The gas saved over the duration of the simulation by a particular LDAR program is the area between the null program time series and the LDAR program time series.

DOI: 10.1021/acs.est.5b06068
Environ. Sci. Technol. XXXX, XXX, XXX−XXX

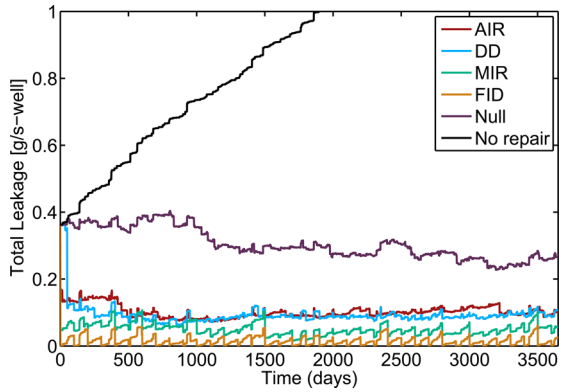

Figure 3. Time series of a single realization of the default scenario in FEAST for the four different LDAR programs, including the null and no-repair programs. In the no-repair case, the total leakage doubles within a few years, while it reaches a steady state in every other case. The null repair scenario fixes the majority of the leaks compared to the no-repair scenario, and therefore, any marginal advantage of the LDAR programs is calculated when compared to the null scenario.

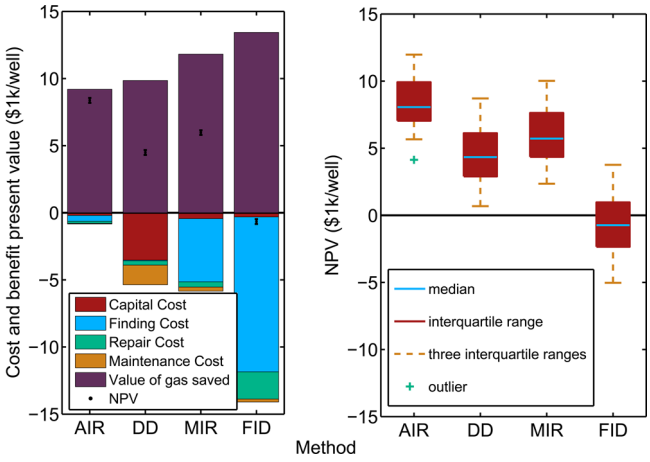

Figure 4. (Left) Variability in the mean behavior between different scenarios of the various LDAR programs shown as a cost versus benefit diagram. Note that the distribution of costs between capital, labor, repairs, and maintenance are dependent upon the technology and methodology adopted in the LDAR program. For example, while the cost of implementing a DD program is dominated by the cost of the detectors, the FID program effectively depends only upon labor costs. (Right) Stochastic variability between different realizations of a scenario for different LDAR programs. While the variation exceeds 50% of the mean in some cases, clear trends can be observed: the FID program, highly dependent upon labor cost, has a significantly lower NPV compared to other LDAR programs.

The null LDAR program is intended to emulate repairs that occur in the field without any explicit LDAR program and is set in this scenario as noted above ($P_{L,R}N_L^i = P_{R,L}N_R^i$). These null program repairs may occur during routine maintenance or upgrades to equipment. We suggest that the null program be used to represent the status quo, although users can choose their own baseline. The no-repair program never removes any leaks from the gas field, and the leakage increases indefinitely ($P_{L,R} = 0$). Because the null scenario repairs the majority of the leaks compared to a no-repair scenario, it is only instructive to compare any marginal advantages of a LDAR program to the null scenario (i.e., no-repair results are not used to calculate LDAR benefits below).

There are two types of variability in FEAST: the variability in the mean behavior between different scenarios and the stochastic variability between realizations. Figure 4 illustrates both of these types of variability. The left panel shows the difference in the mean behavior of the LDAR programs, broken down into cost and benefit components. We can see that the labor cost (a major component of "finding cost") dominates in some technologies (e.g., FID), while the capital cost dominates in others (e.g., DD). The error bars represent the standard error in the estimate of the mean NPV as a result of the limited sample size employed here. The standard error was computed as

$$\sigma_\mu = \frac{\sigma_s}{\sqrt{N}} \tag{7}$$

where σ_μ is the expected standard deviation of the mean in similar samples, σ_s is the sample standard deviation, and N is the number of samples (realizations). In this work, $N = 100$ for each scenario. The variation between stochastic realizations is shown in the right panel of Figure 4. We see that, while the variation between realizations is large, the technologies are different enough that clear trends can be discerned. Considering the median NPV for all realizations, the AIR, DD, and MIR LDAR programs have a positive NPV across the range of inter-realization variability. In comparison to these technologies, the intensive labor costs for a FID-based LDAR program results in a negative median NPV.

Perhaps the most instructive results from FEAST are illustrated by varying scenario settings, as shown in a tornado diagram in Figure 5. The settings used to generate these sensitivity cases are given in Table 2. They were chosen to represent the realistic range of values for each parameter. Note that simulating fields within the realistic range of leak production rates given available data result in enormous variability between scenarios. Clearly, improved data to quantify the leak production rate of gas fields would mitigate the primary driver of uncertainty in FEAST.

One of the base case assumptions in FEAST is a constant leak production rate. Some evidence suggests that gas infrastructure is likely to produce leaks at a greater rate as it ages, although little data exist to quantify this effect in natural gas wells.[10−13] We allow for a variable leak production rate in one sensitivity case: the leak production rate increases linearly from 2.6×10^{-4} g/s per well per day to twice its value over the 10 year simulation period. It can be clearly seen from Figure 5 that any additional increase in the baseline leak creation rate only increases the value of the LDAR programs.

Each LDAR program has unique characteristics that can be adjusted in FEAST to explore their effects. The FID program can be greatly improved by reducing the time required to complete surveys and decreasing the frequency of surveys from the default case. This is because the baseline FID cost is dominated by the labor cost of this slow technology. This result is intuitive because the FID program has no trouble finding leaks and labor is the primary cost of the FID program; reducing the frequency of surveys reduces labor costs more than it decreases gas savings.

In either IR camera program, improving the sensitivity of each camera pixel to methane increases the value of the LDAR programs. However, the results are less sensitive to the number of pixels that must be above the detection limit. Only the MIR program is sensitive to the survey time and survey interval of the program, while the value of the AIR program is largely independent of these factors. In fact, the AIR program is only

DOI: 10.1021/acs.est.5b06068
Environ. Sci. Technol. XXXX, XXX, XXX−XXX

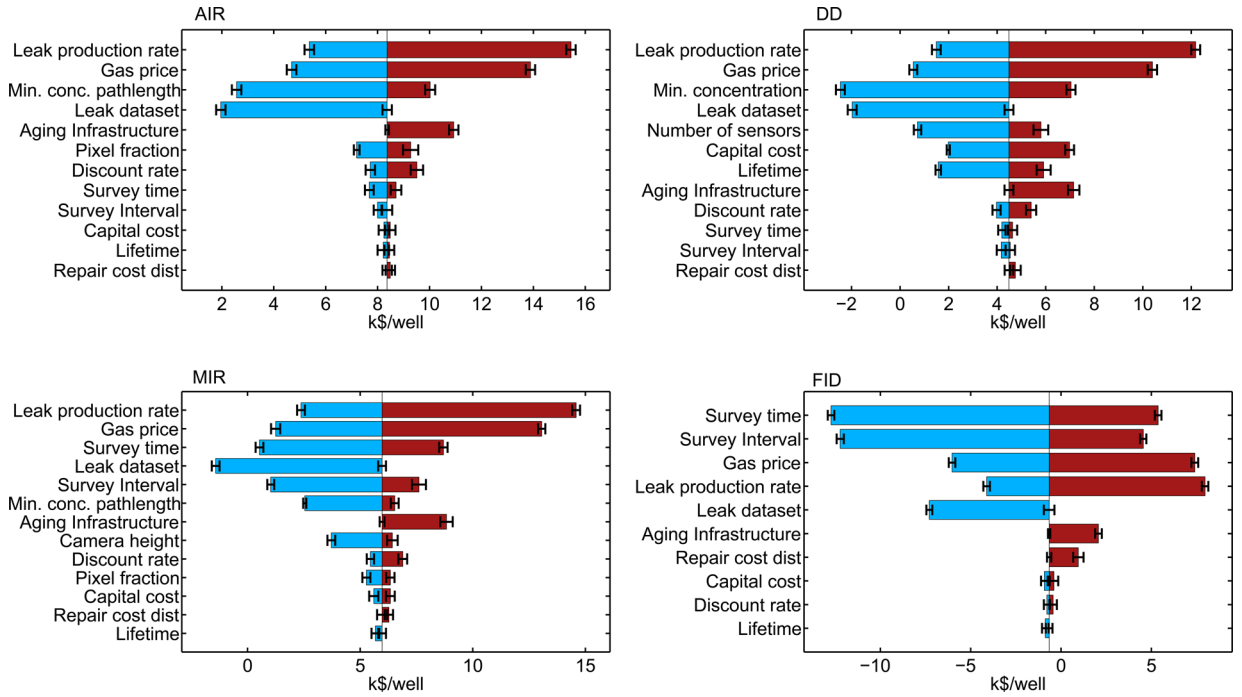

Figure 5. Sensitivity of the NPV of the four simulated LDAR programs to various parameters of the natural gas field, detection technology, and survey procedures. It should be noted that extrinsic factors such as the leak production rate and gas price play an out-sized role in determining the NPV of various LDAR programs. In the case of FID, which has significantly lower NPV than other LDAR programs, we see that reducing the intervals of leak detection will result in a greater cost reduction compared to the reduction in gas savings.

sensitive to properties that affect the number and size of leaks that it detects. This is because the amortized operating costs of the AIR program are very small in comparison to the amount of gas that it detects, as a result of the fact that the automated airborne system can visit a large number of wells per unit time. Reducing the amount of gas detected by 20% has a greater effect on the cash flow of the AIR program than doubling its operating expenses.

The DD program shares many traits with the AIR program: it benefits from changes that increase the number of leaks detected and is insensitive to the survey interval and survey time required to pinpoint the location of leaks. However, the distributed detector program is the only program simulated that is significantly sensitive to the capital cost of the equipment. A distributed detector program requires detectors to be placed at every well, while a single piece of survey equipment for a FID, MIR, or AIR program can service hundreds or even thousands of gas wells, depending upon the survey frequency and time for each survey. Low-sensitivity methane detectors can have extremely low capital costs on the order of $1, but detectors with parts per billion (ppb) scale sensitivity can cost $10 000–100 000. In the base case, we simulated an intermediate detector with a cost of $500 and a sensitivity of 15 ppm.

Notwithstanding the sources of variability in results outlined above, the absolute values computed with FEAST are encouraging. We found that the MIR, AIR, and DD programs are likely to have positive NPVs. Under most scenarios we considered, the AIR program has the greatest NPV, ranging up to $15 000 per well over a 10 year period in the best case sensitivity scenario (see Figure 5).

The most speculative of these scenarios is perhaps the AIR program. Some AIR assumptions may ultimately prove unrealistic. However, the basic characteristics of the program that make it cost-effective are instructive: it allows for high-speed servicing of wells and only identifies relatively large leaks. Sacrificing some sensitivity for speed allows for the majority of leakage to be found (when using realistic heavy-tailed leak size distributions) while greatly reducing operating costs and reducing the cost of fixing small leaks with small gas savings. With these factors included, the capital cost of a drone and high-performance IR camera system (estimated at $193 000 for the purposes of this example) proved to be largely immaterial to the project NPV. This clearly shows that there is a significant divergence between low-cost LDAR technologies ("cheap detectors") and low-cost LDAR programs ("cheap detection"). Low-cost LDAR programs can in fact rely on highly sophisticated and high-cost technology, as long as this technology is applied in a way that allows for rapid scanning and robust detection of large leaks. The end member of such a technology spectrum would be a high-resolution satellite-based system, which would have very high capital costs but could, in principle, detect leaks across a wide swath of the Earth's surface each day.

One of the big challenges in the methane leakage problem is its magnitude; the vast variety in the infrastructure and skewed leak size distribution makes direct measurements and subsequent extrapolation costly (i.e., large sample sizes are needed). Considering the costs associated with implementing leak detection programs, it becomes vitally important to develop tools to help businesses develop cost-effective strategies. FEAST is general enough to allow for businesses and others to tailor the model to specific sites/conditions as they see fit. The results presented here should not be taken as definitive but more as an example of the various possibilities available to users

We emphasize that the economic analysis of various LDAR programs presented here is only indicative of general trends and should not be interpreted as a definitive analysis of the

DOI: 10.1021/acs.est.5b06068
Environ. Sci. Technol. XXXX, XXX, XXX−XXX

cost/benefit ratio for a given technology. Also, FEAST NPV calculations are operator-centric: they take into account the additional revenue from the sale of recovered gas in its cost/benefit analysis but neglect other important effects, such as the social cost of carbon, a future carbon tax or carbon trading market, health benefits associated with the reduction of VOCs, and the avoided costs of climate change adaptation. In proposing new regulations to reduce methane emissions from the U.S. oil and natural gas industry by 40−45% from 2012 levels in 2025, the U.S. EPA has estimated net climate benefits alone at $120−150 million.[28] Adding benefits accrued from reductions in health effects related to fine particle pollution, ozone, and air toxics and improvements in visibility would only incentivize support for a strong methane mitigation policy, resulting in a much higher social NPV for various LDAR programs.

■ ASSOCIATED CONTENT

Supporting Information

The Supporting Information is available free of charge on the ACS Publications website at DOI: 10.1021/acs.est.5b06068.

Simulation code in MATLAB (ZIP)
technical documentation and user guide (PDF)

■ AUTHOR INFORMATION

Corresponding Author

*Telephone: +1-650-724-8251. Fax: +1-650-725-2099. E-mail: abrandt@stanford.edu.

Notes

The authors declare no competing financial interest.

■ REFERENCES

(1) United States Environmental Protection Agency (U.S. EPA). *Inventory of U.S. Greenhouse Gas Emissions and Sinks: 1990−2012*; U.S. EPA: Washington, D.C.. 2014.

(2) Alvarez, R. A.; Pacala, S. W.; Winebrake, J. J.; Chameides, W. L.; Hamburg, S. P. Greater focus needed on methane leakage from natural gas infrastructure. *Proc. Natl. Acad. Sci. U. S. A.* **2012**, *109*, 6435−6440.

(3) Brandt, A.; Heath, G. A.; Kort, E. A.; O'Sullivan, F.; Petron, G.; Jordaan, S. M.; Tans, P.; Wilcox, J.; Gopstein, A. M.; Arent, D.; Wofsy, S.; Brown, N. J.; Bradley, R.; Stucky, G. D.; Eardley, D.; Harriss, R. Methane Leaks from North American Natural Gas Systems. *Science* **2014**, *343*, 733−735.

(4) Advanced Research Projects Agency-Energy (ARPA-E). *Methane Observation Networks with Innovative Technology to Obtain Reductions (MONITOR)*; ARPA-E: Washington, D.C., 2014; http://arpa-e.energy.gov/sites/default/files/documents/files/MONITOR%20and%20DELTA%20Project%20Descriptions_Final_12.15.14.pdf.

(5) Environmental Defense Fund (EDF). *Methane Detectors Challenge*; EDF: Washington, D.C., 2015; https://www.edf.org/energy/natural-gas-policy/methane-detectors-challenge.

(6) Rebellion Photonics. 2015; http://rebellionphotonics.com/.

(7) Kort, E.; Frankenberg, C.; Costigan, K. R.; Lindenmaier, R.; Dubey, M. K.; Wunch, D. Four corners: The largest US methane anomaly viewed from space. *Geophys. Res. Lett.* **2014**, *41*, 6898−6903.

(8) KairosAerospace. http://kairosaerospace.com/.

(9) Mathworks, Inc., *MATLAB, Version 2015b*; Mathworks, Inc.: Natick, MA, 2015.

(10) Gallagher, M. E.; Down, A.; Ackley, R. C.; Zhao, K.; Phillips, N.; Jackson, R. B. Natural Gas Pipeline Replacement Programs Reduce Methane Leaks and Improve Consumer Safety. *Environ. Sci. Technol. Lett.* **2015**, *2*, 286−291.

(11) Fernandez, R. *Cost Effective Directed Inspection and Maintenance Control Opportunities at Five Gas Processing Plants and Upstream Gathering Compressor Stations and Well Sites*; United States Environmental Protection Agency (U.S. EPA): Washington, D.C.. 2006.

(12) Jackson, R. B.; Down, A.; Phillips, N. G.; Ackley, R. C.; Cook, C. W.; Plata, D. L.; Zhao, K. Natural gas pipeline leaks across Washington, DC. *Environ. Sci. Technol.* **2014**, *48*, 2051−8.

(13) Phillips, N. G.; Ackley, R.; Crosson, E. R.; Down, A.; Hutyra, L. R.; Brondfield, M.; Karr, J. D.; Zhao, K.; Jackson, R. B. Mapping urban pipeline leaks: Methane leaks across Boston. *Environ. Pollut.* **2013**, *173*, 1−4.

(14) City of Fort Worth. *Natural Gas Air Quality Study*; City of Fort Worth: Fort Worth, TX, 2011; http://fortworthtexas.gov/gaswells/air-quality-study/final/.

(15) Lyon, D. R.; Zavala-Araiza, D.; Alvarez, R. A.; Harriss, R.; Palacios, V.; Lan, X.; Talbot, R.; Lavoie, T.; Shepson, P.; Yacovitch, T. I.; et al. Constructing a spatially resolved methane emission inventory for the Barnett Shale region. *Environ. Sci. Technol.* **2015**, *49*, 8147−8157.

(16) Brandt, A. R.; et al. Energy and environment. Methane leaks from North American natural gas systems. *Science (Washington, DC, U. S.)* **2014**, *343*, 733−735.

(17) Saunier, S. *Quantifying Cost-effectiveness of Systematic Leak Detection and Repair Programs Using Infrared Cameras*; Carbon Limits: Oslo, Norway, 2014; http://www.carbonlimits.no/wp-content/uploads/2015/06/Carbon_Limits_LDAR.pdf.

(18) Allen, D.; Torres, V. M.; Thomas, J.; Sullivan, D. W.; Harrison, M.; Hendler, A.; Herndon, S. C.; Kolb, C. E.; Fraser, M. P.; Hill, A. D.; Lamb, B.; Miskimins, J.; Sawyer, R.; Seinfeld, J. Measurements of methane emissions at natural gas production sites in the United States. *Proc. Natl. Acad. Sci. U. S. A.* **2013**, *110*, 17768−17773.

(19) Kuo, J. *Estimation of Methane Emissions from the California Natural Gas System*; California Energy Commission: Fullerton, CA, 2012; http://www.energy.ca.gov/2014publications/CEC-500-2014-072/CEC-500-2014-072.pdf.

(20) Bourke, J.; Mire, K.; Newsom, V.; Pike, M.; Ramanan, R.; Shah, A.; Strong, J.; Tixier, C.; Yang, J. *Fugitive Hydrocarbon Emissions from Oil and Gas Production Operations*; American Petroleum Institute (API): Washington, D.C., 1993; 4589.

(21) National Oceanic and Atmospheric Administration (NOAA). *National Weather Service Forecast Office Dallas/Fort Worth, TX Climate Data*; NOAA: Silver Spring, MD, 2014; http://www.srh.noaa.gov/fwd/?n/dfwclimo.

(22) Seinfeld, J.; Pandis, S. *Atmospheric Chemistry and Physics*, 2nd ed.; John Wiley and Sons, Inc.: Hoboken, NJ, 2006.

(23) Pasquill, F. The estimation of the dispersion of windborne material. *Meteorol. Mag.* **1961**, *90*, 33−49.

(24) Gifford, F. A. Use of Routine Meteorological Observations for Estimating Atmospheric Dispersion. *Nucl. Saf.* **1961**, *2*, 47−51.

(25) Beychock, M. *Fundamentals of Stack Gas Dispersion*, 4th ed.; Milton R. Beychok: Irvine, CA, 2005.

(26) Kemp, C. A Simulation Method for Methane Leak Detection and Repair Technologies. Master's Thesis, Stanford University, Stanford, CA, 2015.

(27) Benson, R. G.; Panek, J. A.; Drayton, P. Direct Measurements of Minimum Detectable Vapor Concentrations Using Passive Infrared Optical Imaging Systems. *Proceedings of the 101st Annual Conference & Exhibition (ACE) Meeting of the Air and Waste Management Association*; Portland, OR, June 24−27, 2008; Paper 1025.

(28) United States Environmental Protection Agency (U.S. EPA). Oil and Natural Gas Sector: Emission Standards for New and Modified Sources. *Fed. Regist.*, 2015, *80*, 56593−56698.

DOI: 10.1021/acs.est.5b06068
Environ. Sci. Technol. XXXX, XXX, XXX−XXX